SUPPLEMENTARY INFORMATION

T. F. Leary and A. Ramachandran

1 The interfacial boundary condition for dissolution

For simulating drop dissolution, it is necessary to establish the appropriate boundary condition for dissolution to be imposed at the drop-suspending fluid interface, and determine the ranges of the constants involved in such a condition. As has been the case throughout this paper, all dimensional variables are succeeded by a prime symbol; dimensionless variables do not carry this symbol.

Consider the interface between the drop and the suspending fluid shown in Figure 1. The vector $\mathbf{n}$ is the normal to the interface. The interfacial velocity field is denoted as $\mathcal{V}_I'$. The velocity fields in the drop and suspending fluid phases are $\mathbf{u}'$ and $\mathbf{v}'$ (m/s), respectively, their densities are ρ_u' and ρ_v' (kg/m^3), respectively, and the concentrations of the solute species being exchanged between the drop and the suspending fluid are C_u' and C_v' (mol/m^3), respectively. The drop phase is a pure species, e.g. pure CO_2 or pure SO_2.

An overall mass balance at the drop interface D yields[1]

$$[\rho_u'(\mathbf{u}' - \mathcal{V}_I') \cdot \mathbf{n}]|_D = [\rho_v'(\mathbf{v}' - \mathcal{V}_I') \cdot \mathbf{n}]|_D = 0. \tag{1.1}$$

From a species mass balance, assuming the drop phase a single-component pure species, one gets

$$[C_u'(\mathbf{u}' - \mathcal{V}_I) \cdot \mathbf{n}]|_D = [C_v'(\mathbf{v}' - \mathcal{V}_I') \cdot \mathbf{n}]|_D + k_m'(C_v'|_D - C_\infty'). \tag{1.2}$$

Here, k_m' is the mass transfer coefficient (m/s)[1] corresponding to the transport of the dissolved species from the interface into the bulk suspending fluid.

The above two equations can be solved for the individual velocities of drop phase and outer phase relative to the interfacial normal velocity $\mathcal{V}_I'$.

$$(\mathbf{u}'|_D - \mathcal{V}_I') \cdot \mathbf{n} = \left[k_m' \frac{(C_v' - C_\infty')}{\left(C_u' \frac{\rho_v'}{\rho_u'} - C_v' \right)} \frac{\rho_v'}{\rho_u'} \right] \Bigg|_D . \tag{1.3a}$$

$$(\mathbf{v}'|_D - \mathcal{V}_I') \cdot \mathbf{n} = \left[k_m' \frac{(C_v' - C_\infty')}{\left(C_u' \frac{\rho_v}{\rho_u} - C_v' \right)} \right] \Bigg|_D . \tag{1.3b}$$

The discontinuity in the velocity at the interface is, therefore,

$$[(\mathbf{v}' - \mathbf{u}') \cdot \mathbf{n}]|_D = -k'. \tag{1.4}$$

where

$$k' = k_m' \left[\frac{C_v' - C_\infty'}{C_u' \frac{\rho_v'}{\rho_u'} - C_v'} \left(\frac{\rho_v'}{\rho_u'} - 1 \right) \right] \Bigg|_D \tag{1.5}$$

Eq. 1.4 is boundary condition that has been employed at the interface to simulate dissolution. The constant k' is termed as the dissolution constant, and has units of m/s. In this work, we will use a dimensionless form of the dissolution constant, k, which is defined as

$$k = \frac{\mu' k'}{\gamma'}. \tag{1.6}$$

Here, μ' is the viscosity of the suspending medium, and γ' is the interfacial tension between the drop and suspending fluid.

Let us now estimate the practical range of values of the dissolution constant. For a pure gas dissolving in a liquid, Henry's law allows us to write

$$C'_v|_D = \mathcal{H}' P'. \tag{1.7}$$

where $\mathcal{H}$ is the Henry's law constant in moles of the gas dissolved per m^3 of solution per Pa of pressure. The concentration in the gas phase, C'_u, may be written using the ideal gas law as

$$C'_u = \frac{P'}{R'T'}. \tag{1.8}$$

The ratio of these two concentrations is

$$\frac{C'_v|_D}{C'_u} = \mathcal{H}' R' T'. \tag{1.9}$$

For gases such as carbon dioxide, hydrogen sulphide, sulphur dioxide, and ammonia that are known to be reasonably soluble in water at room temperature (25°C), the Henry's law constants range from 10^{-4} to 10^{-1} mol/(m^3-Pa)^2 . At 25°C, $\mathcal{H}'R'T'$ will range between about 1 to 1000, suggesting that either $C'_v|_D$ and C'_u are of comparable magnitude, or $C'_v >> C'_u$ at the interface. In either case, Eq. 1.5 can be simplified using this result and the fact $\rho'_v << \rho'_u$ for a gas-liquid system, to

$$k' \approx k'_m \mathcal{H}' R' T'. \tag{1.10}$$

Note that the bulk concentration of the gas in the aqueous solution, C'_∞, has been taken to be zero.

The mass transfer coefficient is given by $k'_m = \mathcal{D}'/\delta'$, where $\mathcal{D}' = 1.9 \times 10^{-9}$ m^2/s is the diffusivity of carbon dioxide in water at 25°C, and δ' is the film thickness for mass transfer[3]. Since dissolution experiments are typically carried out in laminar flows in microchannels, the length scale for concentration gradients in the aqueous phase can range between the scale of the microchannel (~ 100 μm) to a few microns. The diffusivity of small dissolved gas molecules in water is of the order of 10^{-9} m^2/s; the mass transfer coefficient, therefore, can vary between 10^{-5} m/s to 10^{-3} m/s. For the ranges of the mass transfer coefficient and the Henry's law constant noted here, Eq. 1.10 suggests that the dissolution constant, k' can vary between 1 μm/s to 10 cm/s.

For typical gas-water interfacial tensions on the order of 10 mN/m, and a medium viscosity of 1 mPa-s, the dimensionless dissolution constant ranges between 10^{-7} to 0.01. For our simulations, we have selected two values from the upper end of this interval representative of strongly dissolving systems, namely $k = 0.001$ and $k = 0.01$. Note that if the interfacial tensions are lowered due to the presence of interfacial species, then k can be larger than 0.01.

Before concluding this section, we make the following note. Dividing Eq. 1.3b by Eq. 1.3a, we get

$$\left[\frac{(\mathbf{v}' - \mathcal{V}'_I)\cdot\mathbf{n}}{(\mathbf{u}' - \mathcal{V}'_I)\cdot\mathbf{n}}\right]\Bigg|_D = \frac{\rho'_u}{\rho'_v}. \tag{1.11}$$

Since $\rho'_v >> \rho'_u$ for gases dissolving in liquids, the above equation indicates that the normal component of the interfacial velocity is closer to the suspending phase velocity than the drop phase velocity. The interface can therefore be advanced in time by employing only the external fluid velocity extracted from the solution of the fluid mechanical model, which is detailed in the next section.

2 Boundary Integral Solutions

The boundary integral formulation used in this work requires expressions to calculate the stress in the outer flow at the tube surface $\mathbf{S}$, as well as an expression for the velocity of the fluid at the drop interfaces $\mathbf{D_l}$ to advance the shapes of the drops with time. The derivation of the boundary integral equations can be found in numerous texts[4–6]. These expressions are defined in terms of the free-space Green's function $\mathbf{G}$ and its corresponding stress tensor $\mathbf{T}$ for a point force in a Stokes flow:

$$\mathbf{G} = \frac{\mathbf{I}}{|\mathbf{x}-\mathbf{x_0}|} + \frac{(\mathbf{x}-\mathbf{x_0})(\mathbf{x}-\mathbf{x_0})}{|\mathbf{x}-\mathbf{x_0}|^3}, \quad \mathbf{T} = -6\frac{(\mathbf{x}-\mathbf{x_0})(\mathbf{x}-\mathbf{x_0})(\mathbf{x}-\mathbf{x_0})}{|\mathbf{x}-\mathbf{x_0}|^5} \tag{2.1}$$

where $\hat{\mathbf{x}} = (\mathbf{x} - \mathbf{x_0})$, the distance between the point force location $\mathbf{x_0}$ and the observation point $\mathbf{x}$. The boundary integral equation for the outer flow $\mathbf{v}$ in the presence of the wall and drop surfaces is:

$$\begin{aligned}\mathbf{v}(\mathbf{x_0}) = \sum_{m=1}^{n} \Bigg[\quad & -\frac{1}{8\pi\mu}\int_{D_m} \mathbf{G}(\mathbf{x},\mathbf{x_0})\cdot(\mathbf{f^v}(\mathbf{x}) - \mathbf{f^u}(\mathbf{x}))dS(\mathbf{x}) \\ & +\frac{1}{8\pi}\int_{D_m} \mathbf{T}(\mathbf{x},\mathbf{x_0})\cdot\mathbf{v}(\mathbf{x})\cdot\mathbf{n}(\mathbf{x})dS(\mathbf{x}) \\ & -\frac{\lambda}{8\pi}\int_{D_m} \mathbf{T}(\mathbf{x},\mathbf{x_0})\cdot\mathbf{u}(\mathbf{x})\cdot\mathbf{n}(\mathbf{x})dS(\mathbf{x})\Bigg] \\ & +\frac{1}{8\pi\mu}\int_{S} \mathbf{G}(\mathbf{x},\mathbf{x_0})\cdot\mathbf{f^v}(\mathbf{x})dS(\mathbf{x}) \\ & -\frac{1}{8\pi}\int_{S} \mathbf{T}(\mathbf{x},\mathbf{x_0})\cdot\mathbf{v}(\mathbf{x})\cdot\mathbf{n}(\mathbf{x})dS(\mathbf{x}) \end{aligned} \tag{2.2}$$

Taking the limit as $\mathbf{x_0}$ approaches $\mathbf{S}$ from the inside of the tube:

$$\begin{aligned}\lim_{x_0\to S^-}\int_S \mathbf{T}(\mathbf{x},\mathbf{x_0})\cdot\mathbf{v}(\mathbf{x})\cdot\mathbf{n}(\mathbf{x})dS(\mathbf{x}) &= -4\pi\mathbf{v}(\mathbf{x_0}\in\mathbf{S}) \\ &+ \int_S \mathbf{T}(\mathbf{x},\mathbf{x_0}\in\mathbf{S})\cdot\mathbf{v}(\mathbf{x})\cdot\mathbf{n}(\mathbf{x})dS(\mathbf{x})\end{aligned} \tag{2.3}$$

Applying 2.3 to 2.2 and rearranging terms:

$$\begin{aligned}\int_S \mathbf{G}(\mathbf{x},\mathbf{x_0}\in\mathbf{S})\cdot\mathbf{f^v}(\mathbf{x})dS(\mathbf{x}) &= 4\pi\mu\mathbf{v}(\mathbf{x_0}\in\mathbf{S}) \\ &+\mu\int_S \mathbf{T}(\mathbf{x},\mathbf{x_0}\in\mathbf{S})\cdot\mathbf{v}(\mathbf{x})\cdot\mathbf{n}(\mathbf{x})dS(\mathbf{x}) \\ &+\sum_{m=1}^{n}\Bigg[\int_{D_m}\mathbf{G}(\mathbf{x},\mathbf{x_0}\in\mathbf{S})\cdot(\mathbf{f^v}(\mathbf{x})-\mathbf{f^u}(\mathbf{x}))dS(\mathbf{x}) \\ &-\mu\int_{D_m}\mathbf{T}(\mathbf{x},\mathbf{x_0}\in\mathbf{S})\cdot\mathbf{v}(\mathbf{x})\cdot\mathbf{n}(\mathbf{x})dS(\mathbf{x}) \\ &+\lambda\mu\int_{D_m}\mathbf{T}(\mathbf{x},\mathbf{x_0}\in\mathbf{S})\cdot\mathbf{u}(\mathbf{x})\cdot\mathbf{n}(\mathbf{x})dS(\mathbf{x})\Bigg]\end{aligned} \tag{2.4}$$

Boundary conditions (4) and (5) (see main text) are applied to produce an expression for the stress in the outer flow $\mathbf{f^{(v)}}$ at the tube surface $\mathbf{S}$:

$$\begin{aligned}\int_S \mathbf{G}(\mathbf{x},\mathbf{x_0}\in\mathbf{S})\cdot\mathbf{f^v}(\mathbf{x})dS(\mathbf{x}) &= 4\pi\mu\mathbf{v}(\mathbf{x_0}\in\mathbf{S}) \\ &+\mu\int_S \mathbf{T}(\mathbf{x},\mathbf{x_0}\in\mathbf{S})\cdot\mathbf{v}(\mathbf{x})\cdot\mathbf{n}(\mathbf{x})dS(\mathbf{x}) \\ &+\sum_{m=1}^{n}\Bigg[\int_{D_m}\mathbf{G}(\mathbf{x},\mathbf{x_0}\in\mathbf{S})\cdot\kappa\mathbf{n}(\mathbf{x})dS(\mathbf{x}) \\ &-(1-\lambda)\mu\int_{D_m}\mathbf{T}(\mathbf{x},\mathbf{x_0}\in\mathbf{S})\cdot\mathbf{v}(\mathbf{x})\cdot\mathbf{n}(\mathbf{x})dS(\mathbf{x}) \\ &+k_m\lambda\mu\int_{D_m}\mathbf{T}(\mathbf{x},\mathbf{x_0}\in\mathbf{S})\cdot\mathbf{n}(\mathbf{x})\cdot\mathbf{n}(\mathbf{x})dS(\mathbf{x})\Bigg]\end{aligned} \tag{2.5}$$

To calculate the velocity on the drop surface $\mathbf{D_l}$, the limit as $\mathbf{x_0}$ approaches $\mathbf{D_l}$ from the exterior is taken for the outer flow and inner flow terms:

$$\lim_{x_0\to D^+}\int_D \mathbf{T}(\mathbf{x},\mathbf{x_0})\cdot\mathbf{v}(\mathbf{x})\cdot\mathbf{n}(\mathbf{x})dS(\mathbf{x}) = 4\pi\mathbf{v}(\mathbf{x_0}\in\mathbf{D_l})$$

$$+ \quad \int_D \mathbf{T}(\mathbf{x}, \mathbf{x_0} \in \mathbf{D_l}) \cdot \mathbf{v}(\mathbf{x}) \cdot \mathbf{n}(\mathbf{x}) dS(\mathbf{x}) \tag{2.6}$$

$$\begin{aligned} \lim_{x_0 \to D^+} \int_D \mathbf{T}(\mathbf{x}, \mathbf{x_0}) \cdot \mathbf{u}(\mathbf{x}) \cdot \mathbf{n}(\mathbf{x}) dS(\mathbf{x}) &= 4\pi \mathbf{u}(\mathbf{x_0} \in \mathbf{D_l}) \\ &+ \int_D \mathbf{T}(\mathbf{x}, \mathbf{x_0} \in \mathbf{D_l}) \cdot \mathbf{u}(\mathbf{x}) \cdot \mathbf{n}(\mathbf{x}) dS(\mathbf{x}) \end{aligned} \tag{2.7}$$

Applying 2.6 and 2.7 to 2.2 and rearranging terms:

$$\begin{aligned} \mathbf{v}(\mathbf{x_0} \in \mathbf{D_l}) = & \sum_{m=1}^{n} \Bigg[-\frac{1}{4\pi\mu} \int_{D_m} \mathbf{G}(\mathbf{x}, \mathbf{x_0} \in \mathbf{D_l}) \cdot (\mathbf{f^v}(\mathbf{x}) - \mathbf{f^u}(\mathbf{x})) dS(\mathbf{x}) \\ & + \frac{1}{4\pi} \int_{D_m} \mathbf{T}(\mathbf{x}, \mathbf{x_0} \in \mathbf{D_l}) \cdot \mathbf{v}(\mathbf{x}) \cdot \mathbf{n}(\mathbf{x}) dS(\mathbf{x}) - \lambda \mathbf{u}(\mathbf{x_0} \in \mathbf{D_l}) \\ & - \frac{\lambda}{4\pi} \int_{D_m} \mathbf{T}(\mathbf{x}, \mathbf{x_0} \in \mathbf{D_l}) \cdot \mathbf{u}(\mathbf{x}) \cdot \mathbf{n}(\mathbf{x}) dS(\mathbf{x}) \Bigg] \\ & + \frac{1}{4\pi\mu} \int_S \mathbf{G}(\mathbf{x}, \mathbf{x_0} \in \mathbf{D_l}) \cdot \mathbf{f^v}(\mathbf{x}) dS(\mathbf{x}) \\ & - \frac{1}{4\pi} \int_S \mathbf{T}(\mathbf{x}, \mathbf{x_0} \in \mathbf{D_l}) \cdot \mathbf{v}(\mathbf{x}) \cdot \mathbf{n}(\mathbf{x}) dS(\mathbf{x}) \end{aligned} \tag{2.8}$$

Boundary conditions (4) and (5) in the main text are again applied to produce an expression for the velocity $\mathbf{v}$ at the drop surface $\mathbf{D_l}$:

$$\begin{aligned} \mathbf{v}(\mathbf{x_0} \in \mathbf{D_l}) = & \frac{1}{4\pi\mu(1+\lambda)} \int_S \mathbf{G}(\mathbf{x}, \mathbf{x_0} \in \mathbf{D_l}) \cdot \mathbf{f^v}(\mathbf{x}) dS(\mathbf{x}) \\ & - \frac{1}{4\pi(1+\lambda)} \int_S \mathbf{T}(\mathbf{x}, \mathbf{x_0} \in \mathbf{D_l}) \cdot \mathbf{v}(\mathbf{x}) \cdot \mathbf{n}(\mathbf{x}) dS(\mathbf{x}) - \frac{\lambda}{1+\lambda} k_l \mathbf{n} \\ & + \sum_{m=1}^{n} \Bigg[- \frac{1}{4\pi\mu(1+\lambda)} \int_{D_m} \mathbf{G}(\mathbf{x}, \mathbf{x_0} \in \mathbf{D_l}) \cdot \kappa \mathbf{n}(\mathbf{x}) dS(\mathbf{x}) \\ & + \frac{1-\lambda}{4\pi(1+\lambda)} \int_{D_m} \mathbf{T}(\mathbf{x}, \mathbf{x_0} \in \mathbf{D_l}) \cdot v(\mathbf{x}) \cdot \mathbf{n}(\mathbf{x}) dS(\mathbf{x}) \\ & - k_m \frac{\lambda}{1+\lambda} \frac{1}{4\pi} \int_{D_m} \mathbf{T}(\mathbf{x}, \mathbf{x_0} \in \mathbf{D_l}) \cdot \mathbf{n}(\mathbf{x}) \cdot \mathbf{n}(\mathbf{x}) dS(\mathbf{x}) \Bigg] \end{aligned} \tag{2.9}$$

Equations 2.5 and 2.9 are the equations used to advance the drop shape with time.

3 Validation of Numerical Method

The results obtained for the case of a single drop with the dissolution rate $k_1 = 0$ are used to validate the numerical method by comparison to the previously published work of Martinez and Udell[7]. Additionally, these results establish the conditions necessary to investigate the effects of drop dissolution without the drop size and the separation distance between drops artificially impacting the results. The tube surface was meshed with 450 uniformly spaced node points and $L = 40$ [see text]. The drop surface was initialized with 300 uniformly-spaced node points, with additional points added when the distance between consecutive node points exceeded the minimum distance between a drop node point and a wall node point. The initial drop shape was specified as a circle for $a < 0.9$ and as an ellipse for $a \geq 0.9$. The drop velocity was initialized as zero.

Fig. 2 shows steady-state values of the drop velocity U_1 as a function of the drop size a for different values of Ca with $\lambda = 1$. When the drop size is very small, U_1 approaches the centerline velocity of the outer fluid, $U_1'/V' = 2$, and is independent of Ca and λ. As the drop size increases, the drop experiences an increased resistance to its motion due to the presence of the wall, and its velocity decreases. For drop sizes $a > 1.1$, the film thickness between the drop and wall reaches an asymptotic value with

respect to a and consequently, so does U_1. The mean fluid velocity across the entire tube must be equal to $\bar{v}$, therefore the smaller the film thickness between the drop interface and the wall, the lower the mean drop velocity U_1. Because the film thickness decreases with decreasing Ca, so does U_1.

When $k_1 = 0$, a steady-state solution to the drop shape that is independent of our chosen inital shape exists for Ca up to 0.8, and the mean velocity of the drop, U_1, becomes constant with time when this shape is achieved (see Supplementary Information-Section 3). For the drop sizes $a > 1.1$ that are the focus of this study, the steady-state shape is characterized by a uniform thickness. This asymptote results from the fact that only the transition regions of the drop at the front and back contribute to the pressure drop in the flow direction, and therefore the length of the film region in the middle of the drop where the axial curvature is zero has no impact on the balance between the interfacial stress and the outer fluid stress[8,9]. The effects of λ and Ca on the steady-state film thickness in this large a asymptote are shown in Fig. 3. The results demonstrate excellent agreement with the work of Martinez and Udell[7].

The distance from the wall at which the outer fluid stress can be balanced by the drop interface is determined by Ca. At large Ca, the interfacial stress is relatively small, and the outer fluid stress pushes the interface farther away from the wall. As Ca decreases, the interfacial stress increases and the stiffer drop surface is able to balance the outer fluid stress at a position closer to the wall. In addition to explicitly defining the relationship between film thickness and Ca, Fig. 3 also demonstrates that larger λ drops have larger film thicknesses due to their ability to balance the shear stress imposed by the outer fluid at a radial position farther from the tube wall where the shear rate is lower. However, note that the film thickness becomes a weak function of λ for $Ca < 0.01$, as was shown by Hodges et al.[9], as the interfacial stress becomes dominant.

To determine the separation distance required to prevent multiple drops in sequence from influencing each other under steady-state conditions, the outer fluid velocity at the tube centerline was evaluated as a function of its distance from the front of a drop at steady-state. The distance from the drop surface at which this velocity reached its ambient value was used as a minimum value for half of the edge-to-edge drop separation distance at which drops were located at the initialization of dissolution. This ensured that changes to the drop shape and velocity were the result of dissolution and not the initial proximity of a sequential drop. As shown in Fig. 4, this minimum distance is nearly independent of Ca and λ.

References

[1] W. M. Deen, *Analysis of transport phenomena*, Oxford University Press, 2012.

[2] R. Sander, *Atmos. Chem. Phys.*, 2015, **15**, 4399–4981.

[3] M. Kreutzer, F. Kapteijn, J. Moulijn and J. Heiszwolf, *Chem. Eng. Sci.*, 2005, **60**, 5895–5916.

[4] C. Pozrikidis, *Boundary integral and singularity methods for linearized viscous flow*, Cambridge University Press, 1992.

[5] L. G. Leal, *Advanced Transport Phenomena*, Cambridge University Press, 2007.

[6] C. Pozrikidis, *J. Fluid Mech.*, 1992, **237**, 627–648.

[7] M. Martinez and K. Udell, *J. Fluid Mech.*, 1990, **210**, 565–591.

[8] F. Bretherton, *J. Fluid Mech.*, 1961, **10**, 166–188.

[9] S. Hodges, O. Jensen and J. Rallison, *J. Fluid Mech.*, 2004, **501**, 279–301.

4 Figures

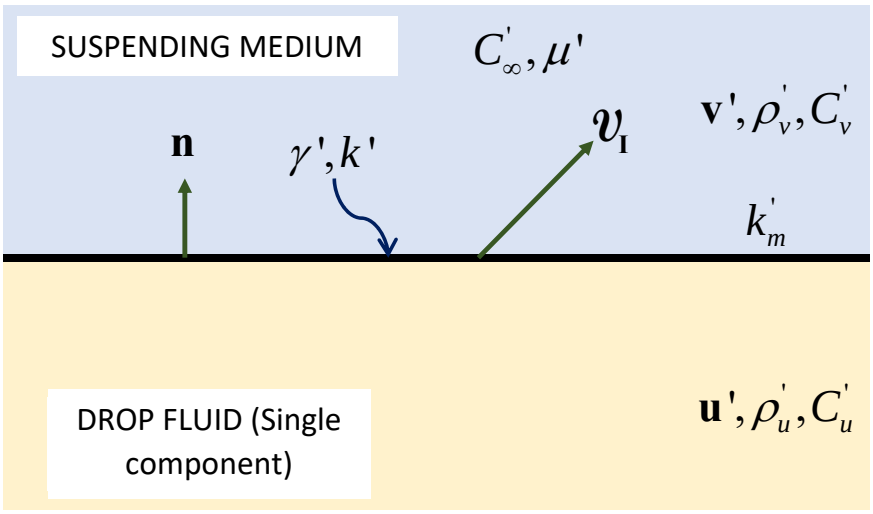

Figure 1 Schematic for the discussion of the interfacial boundary condition for dissolution. The vector vn is the normal vector pointing from the drop phase into the suspending fluid phase. The interfacial tension is γ', and the dissolution velocity of the interface is k'. The velocity field,density and dissolving species concentration in the suspending medium are $\mathbf{v}'$, $\rho_v^{'}$ and $C_v^{'}$, respectively, while the corresponding quantities in the drop phase are $\mathbf{u}'$, $\rho_u^{'}$ and $C_u^{'}$. k_m' is the mass transfer coefficient in the suspending medium. The bulk concentration of the dissolving species in the suspending medium far away from the interface is C_∞. The suspending medium viscosity is μ'.

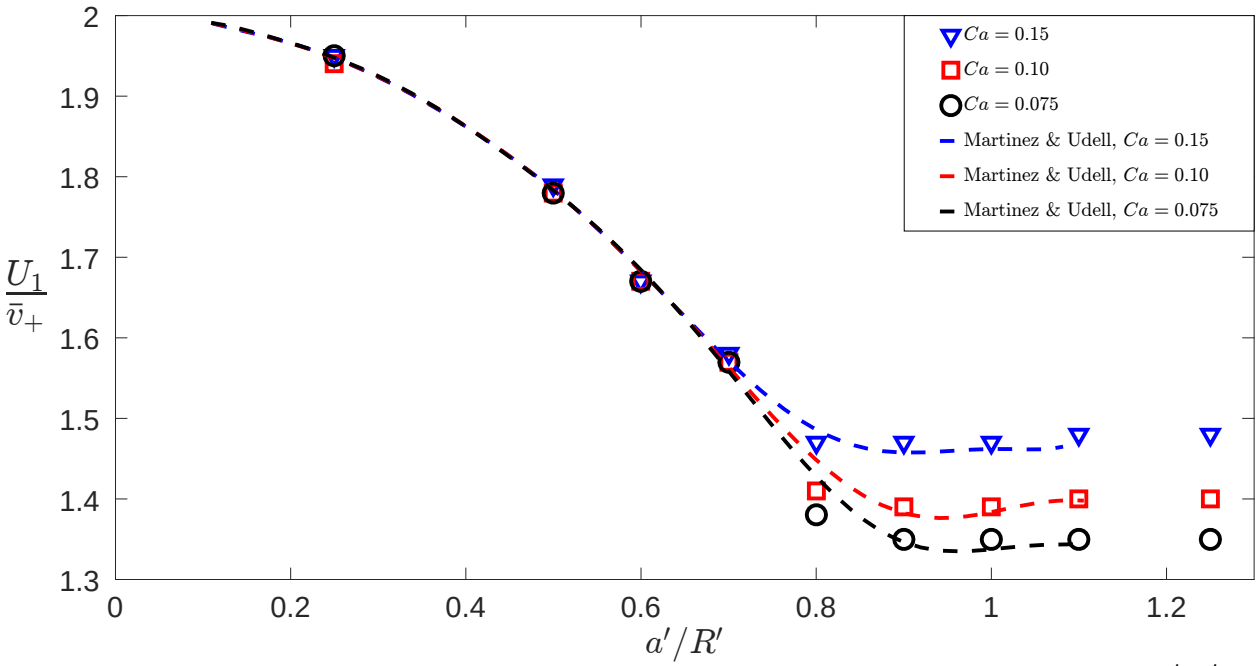

Figure 2 Mean drop velocity U_1 vs. drop size a, $\lambda = 1$, $k_1 = 0$. All drop velocities reach an asymptote with respect to $a = a'/R'$ when $a > 1.1$.

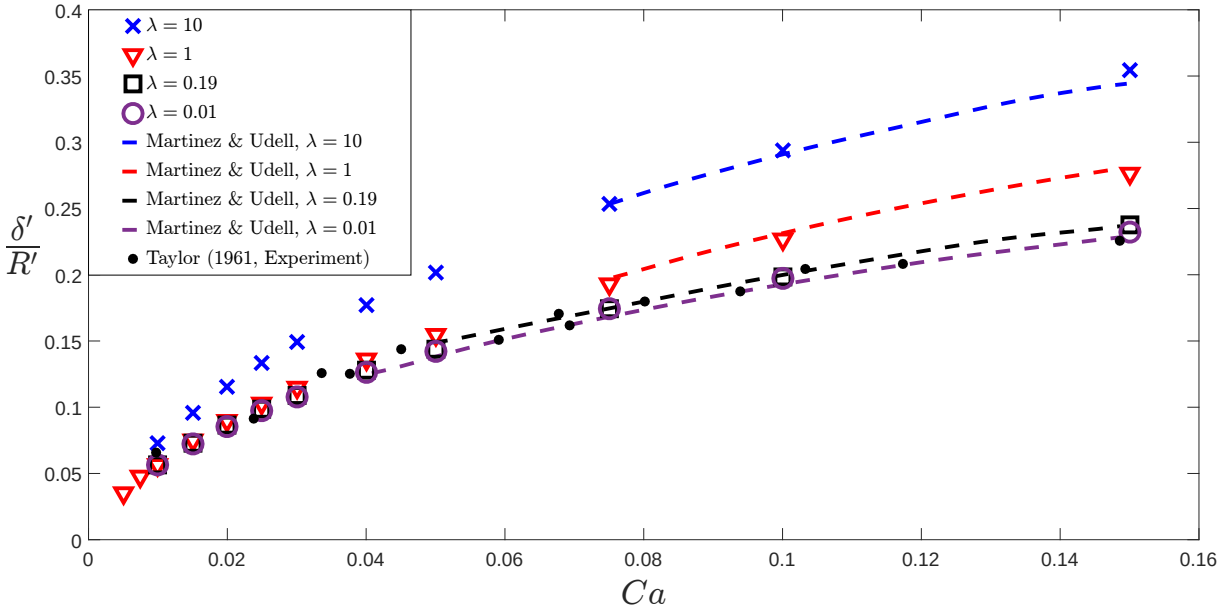

Figure 3 Film thickness vs. capillary number for the large drop size asymptote $a \geq 1.1$.

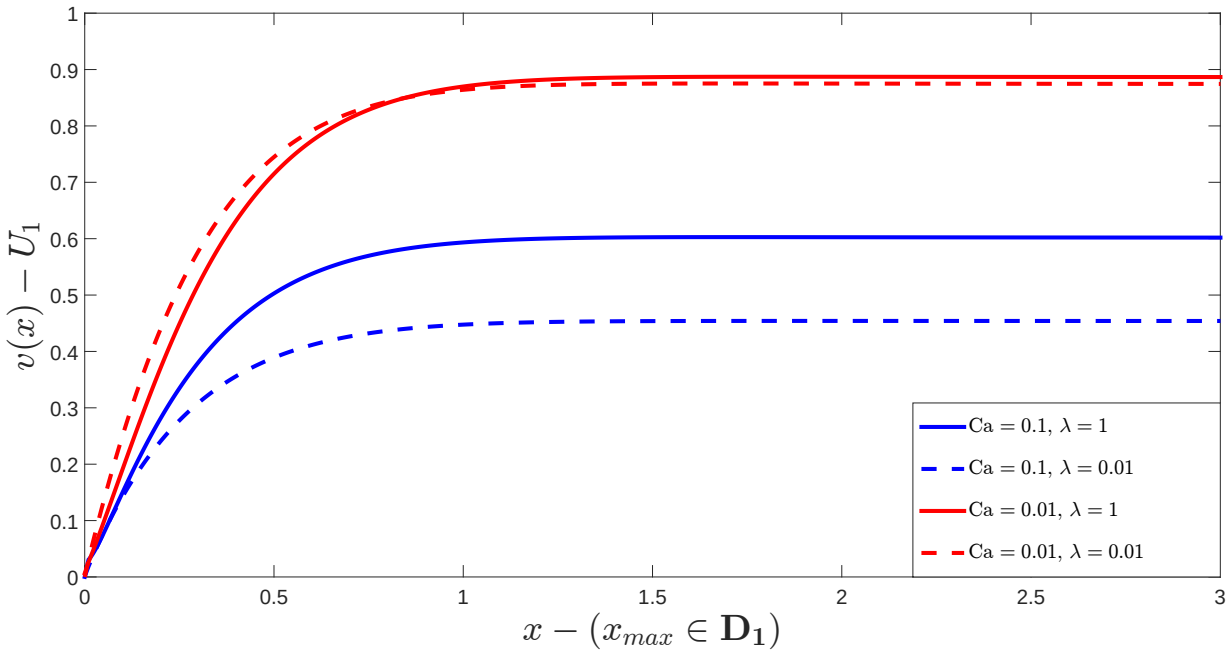

Figure 4 Outer fluid velocity v vs. distance from drop edge at tube centerline, $k_1 = 0$. The deviation from the ambient velocity is less than 0.01% at a distance of 1.5 from the leading edge of the drop; this distance is nearly independent of Ca and λ.